Transformation and Fate of Nanomaterials During Wastewater Treatment and Incineration

Yanjun Ma, Eric P. Vejerano, Jacob Metch , Elena C. Leon, Amara L. Holder, Amy Pruden, and Linsey C. Marr

Civil and Environmental Engineering, Virginia Tech

Blacksburg, VA 24061

ABSTRACT

As the use of nanotechnology in consumer products continues to grow, it is inevitable that some nanomaterials will end up in the waste stream. We assess the transformation and fate of nanomaterials in wastewater and incinerators since these treatment methods have perhaps the greatest potential for transforming nanomaterials. In laboratory-scale sequencing batch reactors (SBRs), nitrification was not inhibited, except when shock-loaded with a high dose of Ag^+ in the influent. Pyrosequencing analysis revealed distinct responses of the microbial community to Ag^+ only and not other nanomaterials, relative to the undosed control. A large portion of nanoAg remained dispersed in the sludge, while nano zero-valent iron (NZVI), nanoTiO_2, and nanoCeO_2 were mostly aggregated. The aggregation state of nanoparticles did not appear to be associated with toxicity. Pure nanomaterials exhibited cytotoxicity and genotoxicity to human lung epithelial cells, but not from the SBR effluents and biosolids. In the exhaust produced by laboratory-scale incineration of paper and plastic wastes loaded with nanomaterials, the particulate matter (PM) size distribution was not affected except at very high mass loadings (10 wt%) of the nanomaterial, in which case the PM shifted toward smaller sizes. Metal oxide nanomaterials reduced emissions of particle-bound polycyclic aromatic hydrocarbons. Generally, nanomaterials had no effect on the toxicity of PM. Most of the nanomaterials that remained in the bottom ash retained their original size and morphology but formed large aggregates. Only small amounts of the nanomaterials partitioned into PM, and the calculated emission factors of nanomaterials from an incinerator equipped with an electrostatic precipitator for control of PM are expected to be low. However, a sustainable disposal method for nanomaterials in the bottom ash is needed, as a majority of them partitioned into this fraction and may thus end up in landfills upon disposal of the ash.

EXPERIMENTAL

WASTEWATER

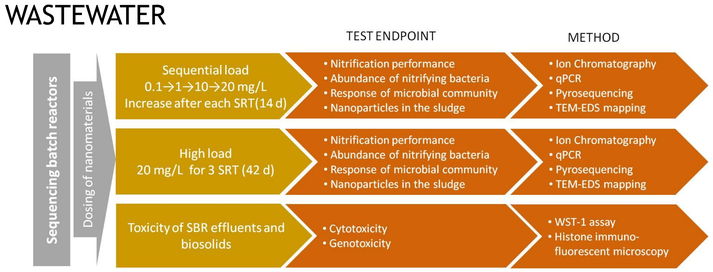

Nanomaterials: nanosilver (particle size 40-60 nm), nano zero-valent iron (30-50 nm), anatase nanoTiO_2 (9- 50nm), nanoCeO_2 (15-30 nm).

INCINERATION

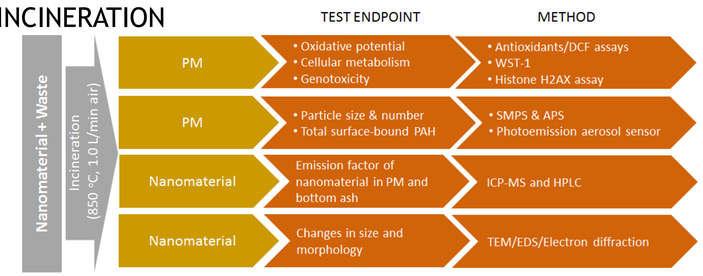

Nanomaterials: anatase TiO_2 (TiO_2, particle size <25 nm, specific surface area 200-220 $m^2\ g^{-1}$), NiO (10-20 nm, 50-80 $m^2\ g^{-1}$), silver (coated with poly(vinyl pyrrolidone), 30-50 nm, 5-10 $m^2\ g^{-1}$), ceria (15-30 nm, 30-50 $m^2\ g^{-1}$), Fe_2O_3 (<30 nm), CdSe/ZnS quantum dots (CdSe QD, <10 nm), and C_{60}. **Waste:** Paper, polyethylene, and PVC at 50 mg each were dosed with 0.1 wt%, 1 wt% and 10 wt% of the nanomaterials.

RESULTS

WASTEWATER

EFFECT ON NITRIFICATION

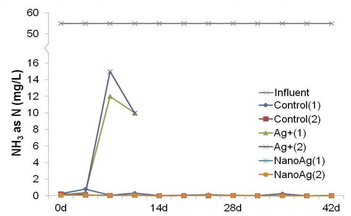

FIG. 1 Accumulation of ammonia in SBRs with high load of 20 mg/L Ag^+. Nitrification function was not impacted in other SBRs.

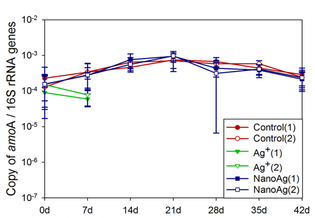

FIG. 2 The abundance of *amo*A gene (a functional gene of ammonia oxidizing bacteria) was significantly decreased in SBRs with high load of 20 mg/L Ag^+.

RESPONSE OF MICROBIAL COMMUNITY

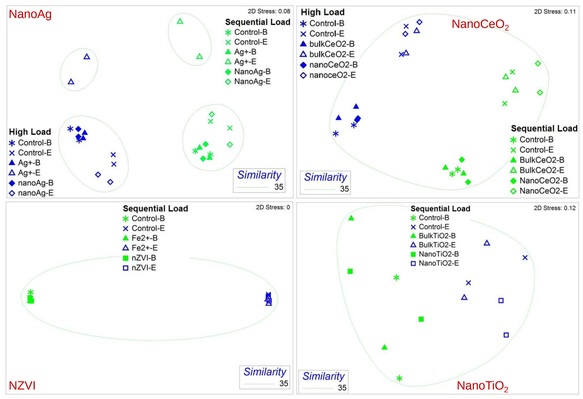

FIG.3 Multidimensional Scaling (MDS) analysis of relative similarities of microbial community compositions before and after dosing in each experiment based on classification of operational taxonomy unit (OUT). SBRs dosed with Ag^+ had distinct microbial communities in both sequential load and high load experiments. No significant difference was observed in SBRs dosed with other nano- or bulk/ionic materials, compared to the undosed controls.

AGGREGATION

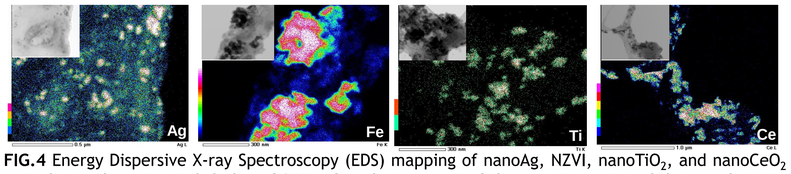

FIG.4 Energy Dispersive X-ray Spectroscopy (EDS) mapping of nanoAg, NZVI, nanoTiO_2, and nanoCeO_2 particles in the activated sludge of SBRs after dosing. Most of the nanoAg remained dispersed. NZVI, nanoTiO_2 and nanoCeO_2 were mostly aggregated. Brighter colors indicate higher X-ray counts.

GENOTOXICITY

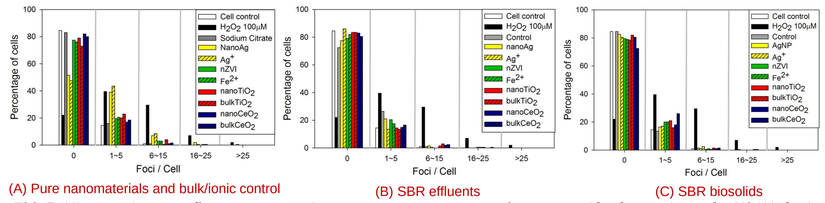

(A) Pure nanomaterials and bulk/ionic control (B) SBR effluents (C) SBR biosolids

FIG.5 Histone immunofluoresecent microscopy assay was used to quantify formation of γH2AX foci formed in A549 lung epithelial cells which indicate double-strand DNA breaks (DSB). Pure nanoAg and Ag^+ showed significant genotoxicity, while no significant difference was observed in other samples compared to control cells.

INCINERATION · AEROSOL CHARACTERIZATION

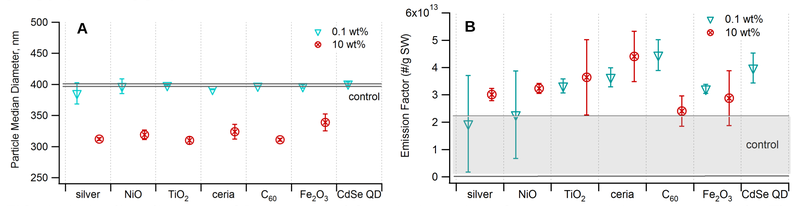

FIG. 6 (A) Median diameter of PM generated from incineration of waste containing nanomaterials. The PM size distribution was not affected except at very high mass loadings (10 wt%) of the nanomaterial, in which case the PM shifted toward smaller sizes. (B) The presence of nanomaterial had no significant effect on particle number emission factor

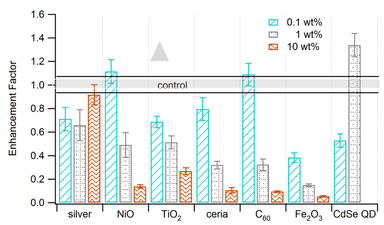

FIG. 7 Enhancement factor of *s*-PAH from the incineration of waste containing various nanomaterials at different mass loadings, relative to the unspiked control, for emission factors (*i.e.*, amount of *s*-PAH emitted per mass of waste burned). Increasing loading of metal oxide nanomaterials and C_{60} decreased *s*-PAH emission.

TRANSFORMATION/PARTITIONING OF NANOMATERIALS

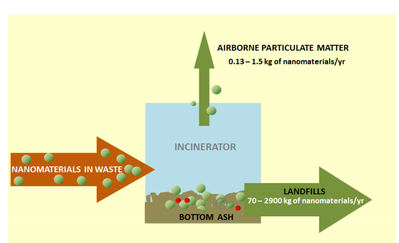

FIG. 8 Emissions of nanomaterial in PM and bottom ash. Assuming that waste consists of 13% nanoproducts containing 0.1 wt% nanomaterials, emissions for a typical municipal solid waste (MSW) incinerator equipped with an electrostatic precipitator and with a daily feed capacity of 100 metric tons are estimated to be 0.13 - 1.5 kg yr^{-1} of nanomaterials, in the flue gas. These emissions represent only 0.021% to 0.25% of the yearly input of nanomaterials entering the incinerator. The largest stream of nanomaterials to the environment from incineration will be the bottom ash.

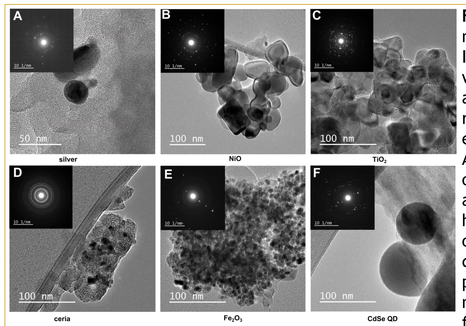

FIG. 9 Representative TEM image of nanoparticles in the bottom ash fraction. (A) Isolated silver nanoparticles. (B) NiO particles were larger than the unburned nanoparticles and did not aggregate. (C) TiO_2 nanoparticles retained their size but appear to be encapsulated and formed aggregates. (D) Aggregate of ceria nanoparticles. (E) Iron oxide nanoparticles also retained their size but aggregated. (F) CdSe QD nanoparticles formed highly spherical nanoparticles larger than the original unburned nanomaterial. The diffraction patterns suggest formation of other phases. Nanoparticles from the original nanomaterial were not detected in the PM fraction.

GENOTOXICITY /CYTOXICITY

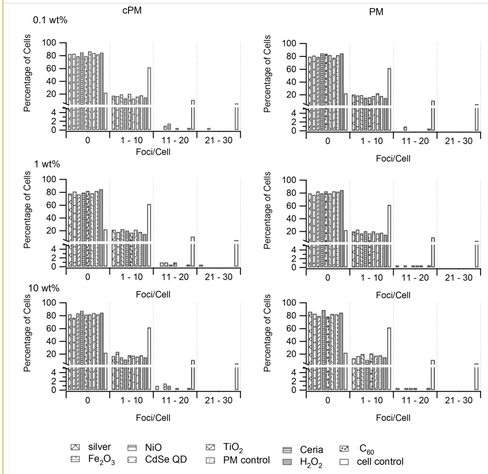

FIG. 10 The genotoxicity of PM appears to be similar to that of the PM from the nanomaterial-free waste in the histone immunofluorescent assay. Similar results for their cytoxicity were observed in the WST-1 assay. (Organic species were removed from cPM using multi-step solvent extraction. PM is the raw aerosol exhaust.)

OXIDATIVE STRESS POTENTIAL

TABLE 1. Difference of means between raw PM (PM) and cleaned PM (*c*PM) for the different assays

	difference of means (|cPM| – |PM|)								
wt%	**0.1**	**1**	**10**	**0.1**	**1**	**10**	**0.1**	**1**	**10**
nanomaterial		**DCF**			**UA**			**AA**	
Silver	-2.8	0.39	-4.6	0.2	-0.2	0.4	-11*	-11*	-15*
NiO	0.31	-2.9	-4.1	-0.2	0.1	0.4	-9..4	-7.5	-16
TiO_2	-2.0	-0.09	-5.6	-0.4	-0.6	-0.4	-15*	-6.5	-11
Ceria	-0.75	-0.14	-5.9*	-1	-0.2	0.1	-7.0	-6.4	-14
C_{60}	-8.0*	-0.54	0.98	-1*	-0.4	0	-8.5	-19*	-14
Fe_2O_3	-5.9*	-0.96	5.0*	-0.7	-0.4	0.2	-7.1	-11	-5.3
CdSe QD	-4.7	-0.68	0.83	-0.6	0.2	-0.4*	-8.7	-14	-34*
PM Control	2.7			0.2			2.0		
		GSH			**GSH/GSSG**			**DTT**	
Silver	-6.3*	-1.1	-0.32	13*	47*	1.2*	19*	14*	23*
NiO	-14	-6.3	5.0	28*	83*	-3.0*	18*	23*	36*
TiO_2	-0.13*	2.8	-0.16	-1.4*	-21*	14*	18*	28*	26*
Ceria	1.6	-2.4	-6.2	5.3*	79*	25*	17*	27*	29*
C_{60}	-1.1	0.30	-5.5	4.6*	4.8*	10*	14*	23*	20*
Fe_2O_3	-24	-7.0*	3.1	16*	14*	0.51*	16*	21*	21*
CdSe QD	-0.49	4.1*	0.17	20*	1.2*	-5.9*	19*	14*	23*
PM Control	0.30			13*			15*		

**significantly different by the Student's t-test at p<0.05*

The oxidative stress potential of PM and *c*PM was unaffected by nanomaterials. For most samples, the oxidative potential of PM and cPM was similar, except in the GSH/GSSG and DTT assays. Results of the dichlorofluorescein assay (DCF) are reported as % fluorescence relative to ethanol. Results for uric acid (UA), ascorbic acid (AA), reduced glutathione (GSH) and oxidized glutathione (GSSG), and dithiothreitol (DTT) are reported as % consumption.

CONCLUSIONS

1) In SBRs simulating a typical nitrifying wastewater treatment process, nanomaterials had no significant impact on nitrification and microbial communities, but Ag^+ did have a significant effect. SBR effluents and biosolids exhibited no significant cytotoxicity and genotoxicity to human lung epithelial cells. We are cautiously optimistic about disposal of nanowaste into wastewater treatment plants, but more studies are needed to verify this interpretation.

2) At mass loadings present in many consumer products, nanomaterials did not affect the size distribution of PM emitted from nanowaste incineration. The particle number emission factor of the PM was higher in the presence of the nanomaterial but not significantly different from that of the nanomaterial-free waste.

3) Nanomaterials in the bottom ash retained their size and morphology, and some nanoparticles became encapsulated. TiO_2, ceria, and Fe_2O_3 formed large aggregates while silver, NiO, and CdSe QD did not.

4) The low level of nanomaterials present in PM coupled with the high removal efficiency of air pollution control devices, if present, implies that the amount released into the atmosphere from an incinerator is expected to be low.

ACKNOWLEDGMENT

Dr. Elankumaran Subbiah and Dr. Chris Winkler

ICTAS INSTITUTE for CRITICAL TECHNOLOGY and APPLIED SCIENCE

This research is funded by U.S. EPA-Science To Achieve Results (STAR) Program Grant # 83485601

VT SUN

NSF

CEINT